Bioorganic & Medicinal Chemistry Letters xxx (xxxx) xxx–xxx

Contents lists available at ScienceDirect

Bioorganic & Medicinal Chemistry Letters

journal homepage: www.elsevier.com/locate/bmcl

Structure activity relationships of anthranilic acid-based compounds on cellular and *in vivo* mitogen activated protein kinase-5 signaling pathways

Suravi Chakrabarty[a,1], Darlene A. Monlish[b,1], Mohit Gupta[a], Thomas D. Wright[b], Van T. Hoang[c], Mitchel Fedak[d], Ishveen Chopra[a], Patrick T. Flaherty[a,*], Jeffry Madura[d], Shankar Mannepelli[d], Matthew E. Burow[c], Jane E. Cavanaugh[b]

[a] Department of Medicinal Chemistry, School of Pharmacy, Duquesne University, 410A Mellon Hall, 600 Forbes Ave., Pittsburgh, PA 15282, United States
[b] Department of Pharmacology, School of Pharmacy, Duquesne University, 410A Mellon Hall, 600 Forbes Ave., Pittsburgh, PA 15282, United States
[c] Department of Medicine-Section of Hematology and Medical Oncology, Tulane University, New Orleans, LA 70118, United States
[d] Department of Chemistry, Duquesne University, 410A Mellon Hall, 600 Forbes Ave., Pittsburgh, PA 15282, United States

Cancer comprises of a group of heterogeneous diseases; increasingly it is recognized that upregulation of mitogenic pathways occur early during the process of disease progression. The mitogen-activated protein kinase (MAPK) signaling cascade is a complex web of signaling events that mediate appropriate intracellular responses to external mitogenic events.[1] This highly branched signaling cascade possesses a singular parallel processing stage where each ERK (extracellular signal-regulated kinase) is phosphorylated uniquely by its corresponding MEK (MAPK/ERK kinase). Enzymatically, MEKs belong to the serine/threonine kinase[2] family. A recent metabolomics study suggests that the biochemical outcome resulting from this three-tiered kinase cascade strategy is a more rapid yet adaptable cellular response. Genomic analysis indicates that this 3-teired kinase cascade strategy[3,4] is carefully conserved across species and represents a signaling strategy of sustained biological relevance. Cross-talk between the pathways is guided by a variety of mechanisms including controlled sub-cellular localization of kinase isoforms, activation by enzyme-catalyzed phosphorylation events, and protein-protein association directly between the kinases as well as associations involving platform proteins as well.

In a recent review of the MAPK pathways,[5] careful analyses was directed at the MEK1/ERK1 and MEK2/ERK2 pathway. The role of other MEK pathways, specifically the MEK5/ERK5 pathway remains less than thoroughly understood due to the lack of small molecule probes.[5]

A compelling case has been presented for the role of MEK5 in various cancers.[6–8] Major techniques to analyze contributions of each MEK/ERK pathway entail a combination of small molecule probes as well as gene manipulation strategies. These approaches have limitations. Gene manipulations are often cell-line specific. The best-characterized inhibitor of the MEK5/ERK5 pathway is XMD8-92.[9–11] This compound is an ATP-site inhibitor of ERK5. Interception at earlier step in the kinase cascade could potentially offer a greater impact and higher selectivity.[6] Additionally, the capacity for ERK5 to exist either as cytosolic or nuclear protein and to have multiple post-translational phosphorylation states (pT219, pY221, pS720, and pT733)[11] complicates the understanding of the effects of the MEK5/ERK5 cascade by targeting downstream components such as ERK5. For example, phosphorylation of ERK5 at THR732 is associated with translocation to the nucleus.[12,13] This is not a MEK5 mediated event: MEK5 phosphorylates Thr219[12] of the TEY sequence (219-221).

To date, ERK5 is the only known substrate for MEK5; therefore, targeting this unique pathway at MEK5 may minimize side effects and reduce toxicity by sparing other MAP kinase events critical for the homeostasis and survival of healthy cells. The MEK5/ERK5 pathway mediates effects of several oncogenes,[7] including Ras and Src but further understanding of this cascade is required.[14–17] The MEK5/ERK5 pathway is constitutively active in numerous cancer types.[1] MEK5 is overexpressed in over 50% of tumors analyzed and ERK5 is elevated in over 20% of patients. Significantly, elevated ERK5 expression reduces disease-free survival time of breast cancer patients compared to patients with lower expression levels of this kinase.[18,19] The development of small molecule modifiers of the MEK5/ERK5 MAPK pathway is necessary to understand the MEK5/ERK5 pathways in various cell types and to explore potential drug intervention strategies.

Development of inhibitors of the MEK1/2 isoform employed X-ray crystal based compound design preceding from the discovery that active substituted *N,N*-diphenylanilines do not bind at the ATP site, but instead bind to a hydrophobic site proximal to the ATP-associated Mg^{2+} ion site near the C helix.[20,21] This site has been exploited extensively in the development of MEK1/2 inhibitors and has generated two recently FDA-approved drugs: mekinist® (trametinib) and cotellic® (cobimetinib). This site is now termed the type III inhibitor binding site[2,22] and its presence and relevance to drug design has been confirmed in other protein kinases.[23] Ligand binding to the type III site

* Corresponding author.
E-mail address: flahertyp@duq.edu (P.T. Flaherty).
[1] These authors contributed equally to this work.

https://doi.org/10.1016/j.bmcl.2018.05.029
Received 14 December 2017; Received in revised form 11 May 2018; Accepted 12 May 2018

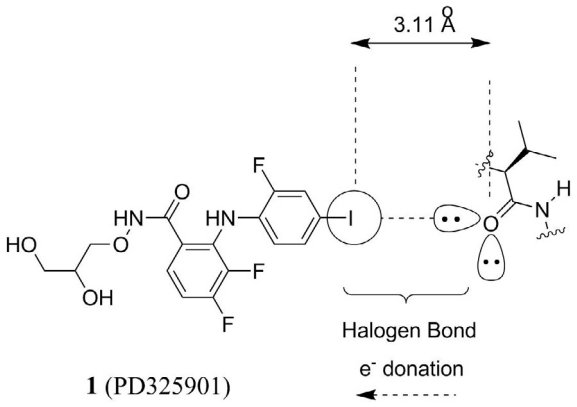

Fig. 1. Schematic of halogen bond from the 4′-iodo atom **1** (PD325901) to the lone pair of the acyl of Val in 3EQC.[24]

prevents phosphorylation of a given MEK by the associated upstream MEKK (MEK-kinase) and consequently prevents activation of a given MEK. Considerable effort has been directed toward developing type III MEK1/2 inhibitors. For all MEK1/2 inhibitors in the literature there is a rigorous requirement for a halogen substitution on the terminal arene at the para position. The 2-F, 4-I arene substitution pattern exists in the original compound **1**, PD325901 found in the X-ray crystal structure[21] of MEK 1 (PDB ID: 3EQC), as well as for all FDA-approved MEK1/2 inhibitors (trametinib and cobimetinib). In most pre-clinical SAR studies the 4-iodo moiety is stated as essential for MEK1/2 activity.[21] The 3.11 Å distance from the lone pair of electrons from the backbone amide acyl of Val127 to the iodine atom in the X-ray structure 3EQC[24] displayed in Fig. 1 is consistent with a halogen bond.[25–29]

A 4′-iodine atom on the terminal arene is essential for MEK1/2 activity. Additional examination of 3EQC indicates that the iodine atom fills a large hydrophobic pocket. This hydrophobic pocket is non-identical between MEK1 and the pocket proposed by the homology model of MEK5 (see below). The central arene ring is tolerant of wide variability for MEK1 inhibitors. Extension of the central arene ring to a benzo-fused heterocycle has also been explored.[30] These heterocyclic ring variations have displayed a capacity to act as a hydrogen bond partners with Ser212 on the C-helix. Side-chain variations from the central benzamide have successfully been explored to yield potent inhibitors of MEK1[30] with an emphasis on designing better PK properties than present in **1**. An analog design approach informed by both existing MEK1 SAR and structure-informed design based on multiple MEK5 homology models explored substitution patterns on the arene rings and the amide sidechain with the goal of optimizing MEK5 potency and selectivity.

There has been significant analysis of the structure of MEK1; there are 39 X-ray crystal structures of MEK1 with resolutions ranging between 2.93 Å and 1.8 Å with 50% obtained at 2.5 Å resolution or better. There is less known about the other isoforms. MEK2 is represented by 1 structure. MEK6 is represented by 3 structures containing the kinase domain. MEK7 is represented by 5 structures containing the kinase domain. The kinases MEK3, MEK4, and MEK5 do not have any X-ray crystal structures with kinase domains deposited in the PDB. There are three structures for wild type and mutant *N*-terminal PB1 domains of MEK5 deposited (residues 5–10 and 16–130)[31], but none contain the kinase domain found in residues 166–409. The MEK5 structures deposited examined trimeric protein-protein interactions between MEK5 fragments, ERK5, and MEKK3. A sequence homology tree, shown in Fig. 2, identified MEK5 as being most similar to MEK1 and MEK2 when compared to all possible MEK isoforms.[31]

Several homology models were constructed on the structure of MEK1 (3EQC).[32] The bound ligand is a type III inhibitor. The canonical beta isoform[33–35] of MEK5 (Uniprot: Q13163) with 448 amino acid residues was chosen for sequence to be used for the homology model.

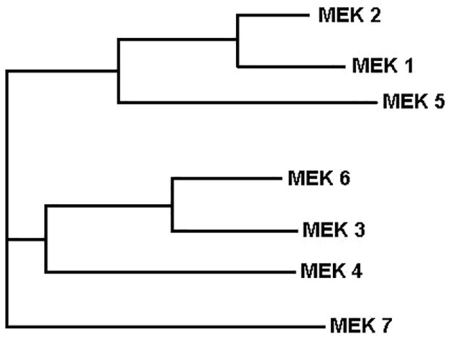

Fig. 2. Phylogram analysis of MEK isoforms; MEK5 is most closely related to MEK1 and MEK2.

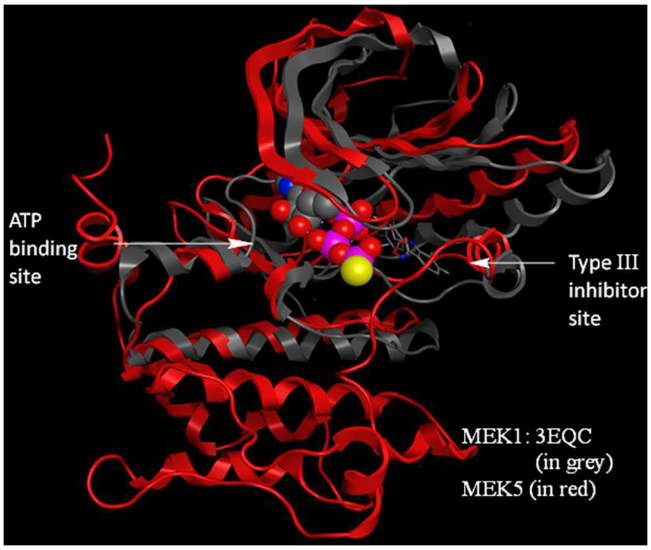

Fig. 3. ATP and Type III binding sites of the MEK1 crystal structure (PDB ID: 3EQC) superimposed on a homology model of MEK5. ATP is shown as space filling and **1** is shown as a stick representation in the proposed type III binding site.

Multiple models representing the DFG-in and the DFG-out conformations, as well of the various phosphorylated forms were examined. Both Accelrys Discovery Studio and MOE 2009.10 were used to examine the proteins and ligand interactions. Docking was conducted with side-chain flexibility for residues lining and adjacent to the proposed type III binding domain (See Fig. 3).

The *N,N*-diphenylaniline moiety was selected as the core structure to be elaborated because it exists in the PD325901 structure, provides rapid synthesis of analogs, and permits structural variation at locations that interact with the proposed type III pocket. The modifications examined are presented in Fig. 4.

Desired biological consequences of structural modification include both PD and PK effects. Specifically, providing either ionization or increased hydrogen bonding on the side chain lowers the cLogP and provides the potential to interact the more polar lip of the P-loop. This region is normally associated with ATP triphosphate transfer and is the same location were the glycerol portion of **1** binds to MEK1. This region in the MEK5 homology models also displays a very polar domain with subtle variations that could offer differential affinity for MEK5 versus MEK1 or MEK2. Specifically Asp283 of the MEK5 HRD sequence is proposed to correlate with Asp 190 of the HRD sequence of MEK1. Although these regions are close in the overlay of the two models, they differ by at least 2 Å and form the bottom of the ATP binding site adjacent to the Type III binding pocket. Also, the C-helices near the ATP binding site are non-identical; the MEK5 Tyr315 residue of the YVGT

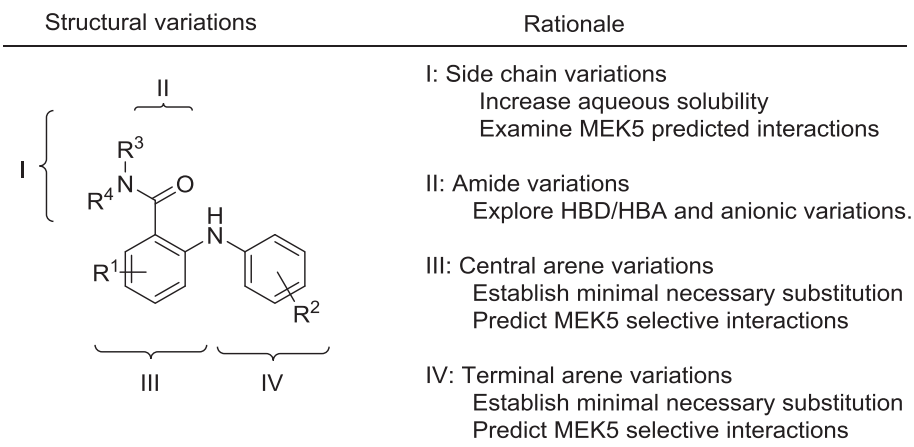

Fig. 4. Side chain variation and amide variations and rationale.

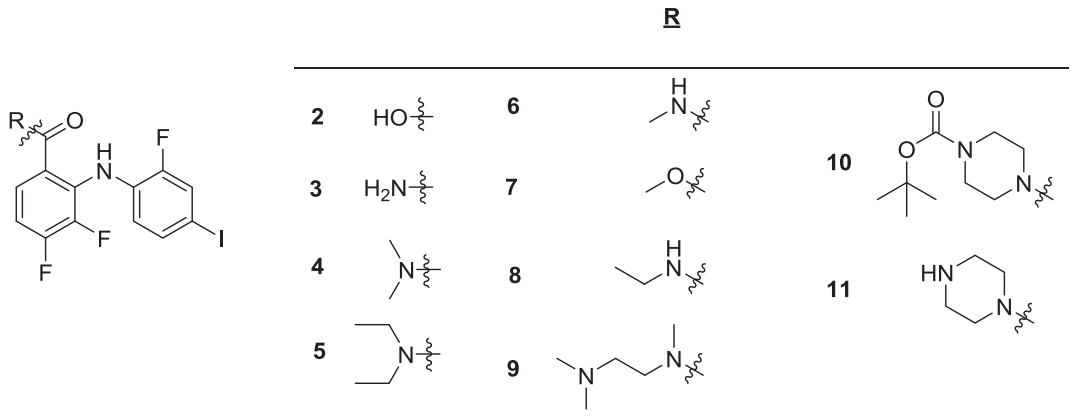

Fig. 5. Proposed side chain variations.

corresponds to the MEK1 Phe223 residue of the FVGT sequence. Variations of basic amine placement and alteration of flexibility were proposed to explore this area. Given the flexibility of the P-loop geometry relative to the lower α-helical domain, multiple variations were examined as shown in Fig. 4. Sidechain variations examined also included synthetic precursors (amides, acids, *tert*-butyl carbamates) and characterized side-products (See Fig. 5).

Prior literature[36] indicated that the 3 and 4 fluorine atoms of the central arene ring, present on the lead compound **PD325901**, functioned as more than just electron-withdrawing groups. It has been proposed that the 4-fluorine atom, can form an electrostatic or hydrogen/halogen bond interaction with the Ser212 of the C-helix in the MEK1 structure. With an eye toward eventual replacement of the central arene, an initial survey of the requirement and utility of 3,4-difluorine substitution on the central arene for MEK5 inhibition was conducted and is presented in Fig. 6.

Terminal arene variations were prepared to survey the need and utility of fluorine and iodine atom substitution for MEK5 inhibition. Of particular note, the 4′-iodine atom presented multiple sub-ideal chemical features: high molecular weight (126 Da), large hydrophobic area, and potential photo-instability. Despite these disadvantages, the 4′-iodophenyl moiety is scrupulously retained in all compounds in advanced MEK1 inhibitors and both FDA approved MEK1/2 inhibitors. Point variations in Fig. 7 were examined with the goals of decreasing MEK1/2 activity and increasing MEK5 activity.

Internal hydrogen bonding from the aniline proton to the acyl oxygen lone pair of the amide is predicted by deposited X-ray crystal structures of MEK1/2 type III inhibitors. These structures display an unvarying presence of secondary amines at this position. The geometry of the heavy atoms identified in the deposited X-ray crystal structures is

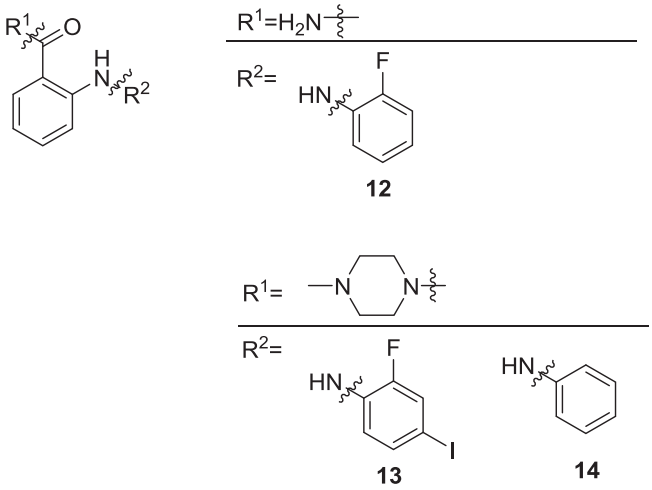

Fig. 6. Central unsubstituted aryl derivatives and associated right aryl and side-chain variants.

consistent with internal hydrogen bonding resulting in a 6-membered ring as shown in Fig. 8. It is unclear if this internal bond from the aniline NH to the acyl lone pair is necessary or useful for MEK5 inhibition. The *N*-methyl-*N,N*-diphenylaniline analogs, compounds **21–24** in Fig. 9 are unable to participate in internal H-bonding and were prepared to examine the contribution of internal hydrogen bonding toward MEK1 and MEK5 activity.

The synthesis of these compounds proceeded by initial formation of the *N,N*-diphenylaniline followed by subsequent conversion of the

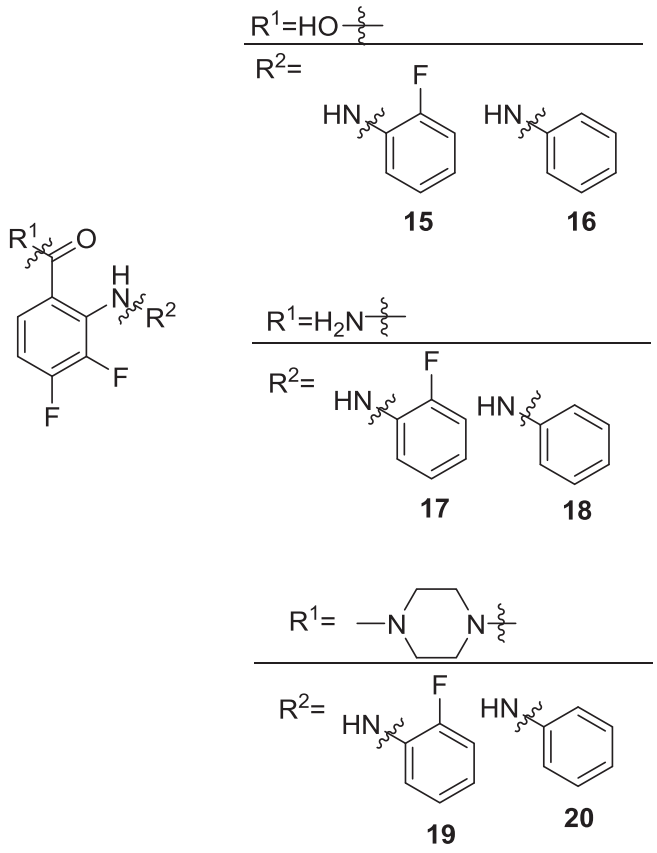

Fig. 7. Right aryl derivatives and associated side-chain variants.

benzoic acid to the desired amide. *N,N*-Diphenylaniline are typically synthesized with a copper-catalyzed Ullmann coupling[37–44] or in the case of a 3,4-difluoro substitution pattern on the central ring, they can be prepared by directed nucleophilic attack of the lithium salt of the terminal aniline. This attack into the strongly electron deficient central arene ring was explored by Davis[45] and found to proceed well with analogous strongly electron-deficient rings. For the central arene without halogens, an Ullmann coupling was successfully employed. Conversion of the benzoic acid to the desired amide could generally be achieved by routine conversion to the intermediate acyl chloride with oxalyl chloride/DMF then use of excess amine. This proceeded well when the arenes contained halogens, but in the case of unsubstituted arenes, this strategy failed. This was attributed to self-condensation of the less-electron deficient anilines with the acyl chloride. In such cases, lower temperature carbodiimide couplings[46] were successfully used.

Synthesis of the 3,4-difluoro-*N,N*-diphenylaniline core, **2**, at a multigram scale was previously achieved using the lithium salt of the terminal aniline displacement shown in Scheme 1 and developed by Davis et al.[45]

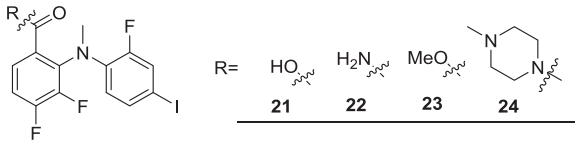

Fig. 9. *N*-Methyl derivatives designed to explore the necessity of internal H-bonding.

Preferential substitution occurs at the *ortho*-position as identified in the literature. Davis et al.[45] proposed the lithium carboxylate of **25** coordinates with and directs the lithium salt of **26** towards the *ortho*-position of the carboxylate to facilitate nucleophilic attack at the 2-carbon bearing a fluorine shown as **27** in Scheme 1. The 2-carbon of compound **25** is the most electron deficient carbon atom due to the attached fluorine atom, an adjacent fluorine atom, and most significantly the *ortho* carboxylate. Inductive effects are decreased by the inverse square of distance encouraging selective nucleophilic attack at the 2-carbon. This method has been used previously to prepare compounds that were co-crystallized in the structure of MEK1 confirming the regioselectivity of the addition. The ^{1}H NMR and physical properties for the current synthesis were identical with the literature.[45] This general approach was subsequently explored for ring variations as described below.

The acid, **2**, was readily converted into the corresponding acid chloride in 2 h at ambient temperature by oxalyl chloride and catalytic DMF in dichloromethane as shown in Scheme 1. The crude acid chloride, **28**, was added directly to an excess of the appropriate amine.

Synthesis of the desired unsubstituted central arene benzoic acids **32–33** were not formed by S_NAr chemistry from the lithium salt of the aniline due to absence of fluorine atoms and resultant decrease in electrophilicity of the 2-carbon of the benzoate. An Ullmann coupling between **2** and iodobenzoic acid, **29**, and amines **26**, **30**, and **31** gave the desired acids **32–34** in acceptable isolated yield (typically ~ 50%). Recent Ullmann coupling variations[47–51] recommended conditions shown in Scheme 2. The best conditions used were copper iodide, potassium carbonate, and a mixed solvent system of 9 to 1 DMF to water with microwave irradiation.

Conversion of the benzoic acids **32–34** to the corresponding amides was achieved with oxalyl chloride/dimethyl formamide route as previously described followed by excess amine to give the desired amides **12** and **13**. Compound **14** could not be prepared efficiently by the acid chloride method. Use of standard DIC (diisopropylcarbodiimide) coupling gave **14** in acceptable yield. A rationalization for the failure of the acid chloride strategy is probable self-condensation; the absence of halogens in compound **34** renders the nitrogen atom less electron deficient than previous *N,N*-diphenylanilines examined.

Desired compounds retaining the central 3,4-difluoro-substitution pattern with variations on the terminal arene as well as the side chain variants were effectively prepared by S_NAr of an appropriately substituted lithium amide. Fewer electron-withdrawing groups on the terminal aniline did raise the pKa, but lithium amide was an adequate

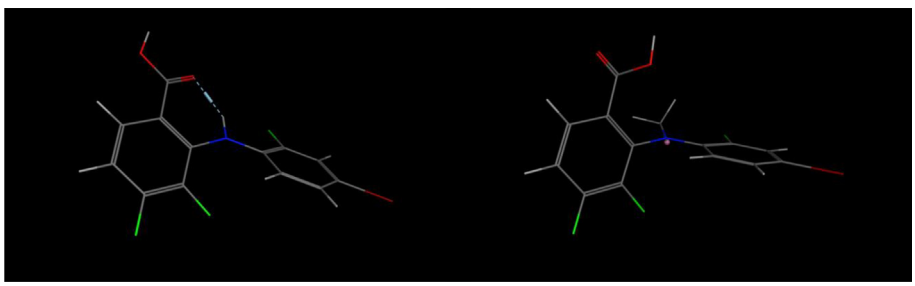

Fig. 8. Internal hydrogen bonding results in a more conformationally restricted analog (compound **2**, left); the *N*-methyl in compound **21** prevents internal hydrogen bonding and results in a less conformationally restricted structure.

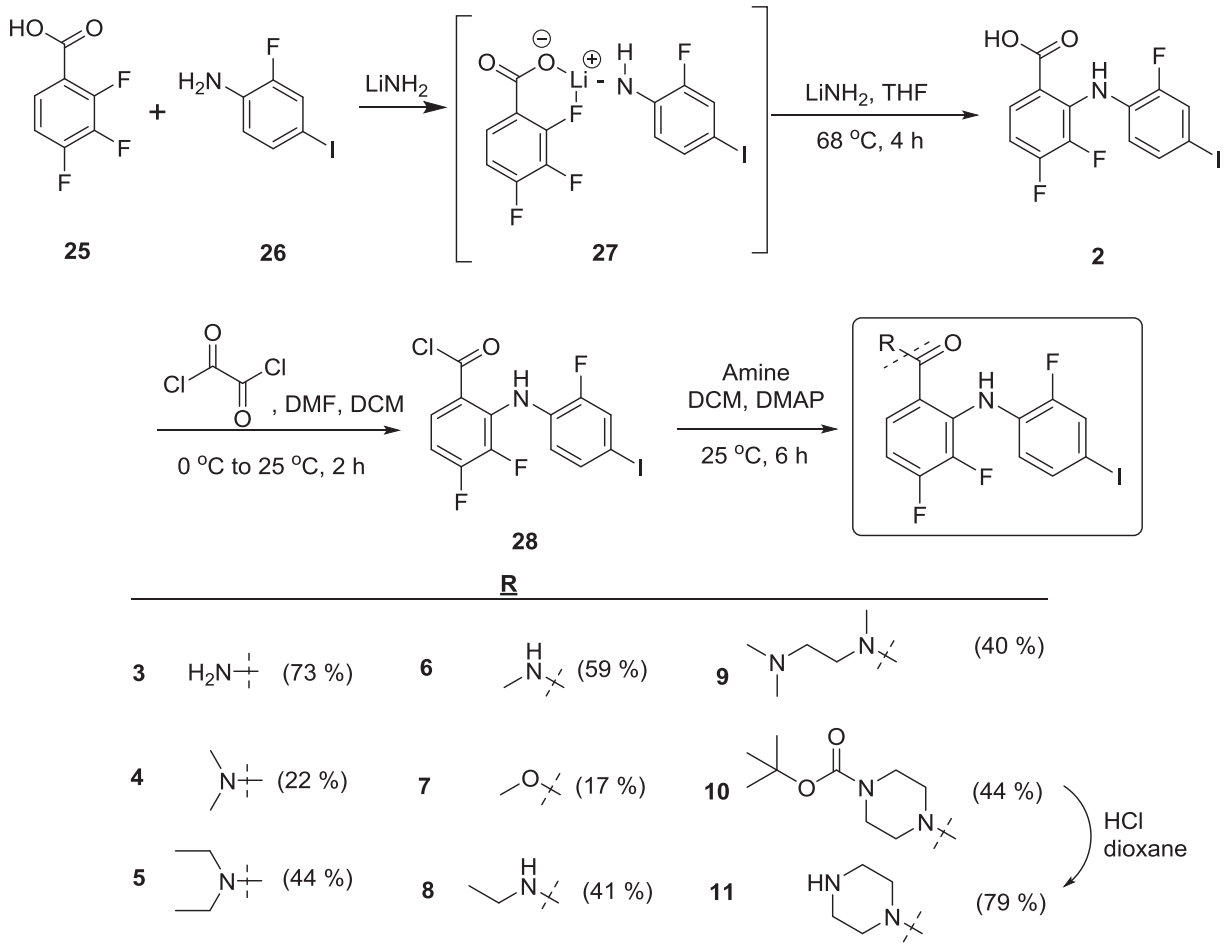

Scheme 1. Synthesis of amides using the acid chloride method from the lithium salt of aniline **26**.[45]

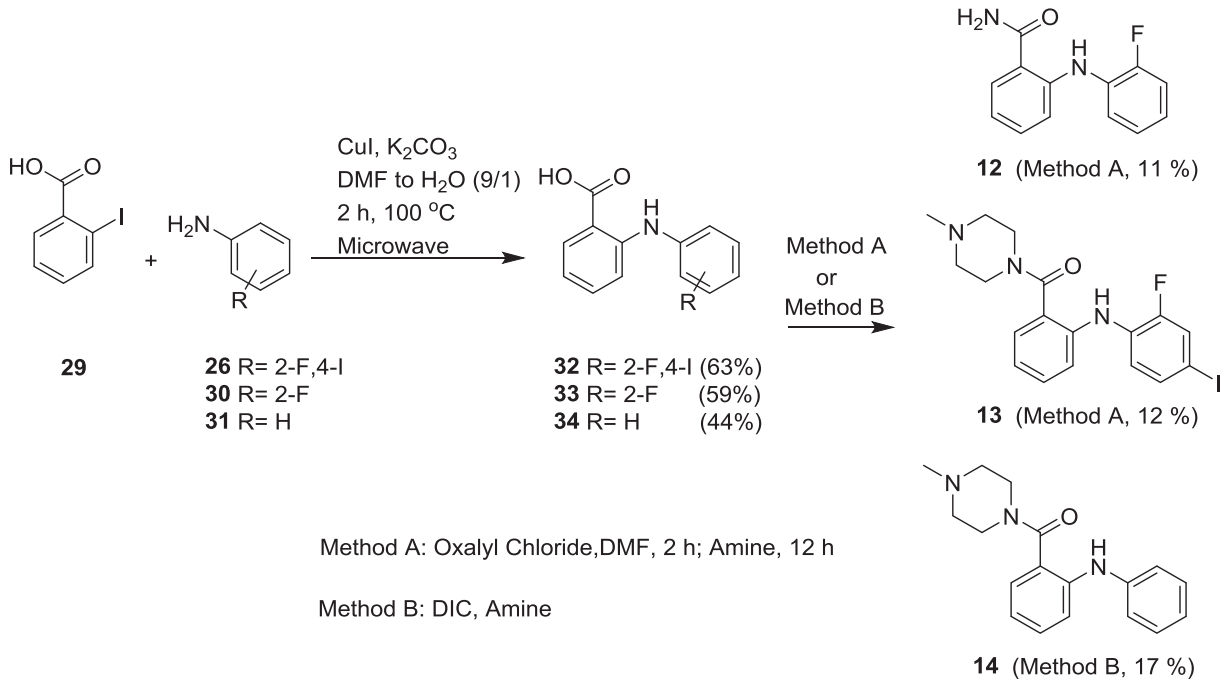

Scheme 2. Synthesis of central unsubstituted aryl derivatives and associated right aryl and side-chain variants.

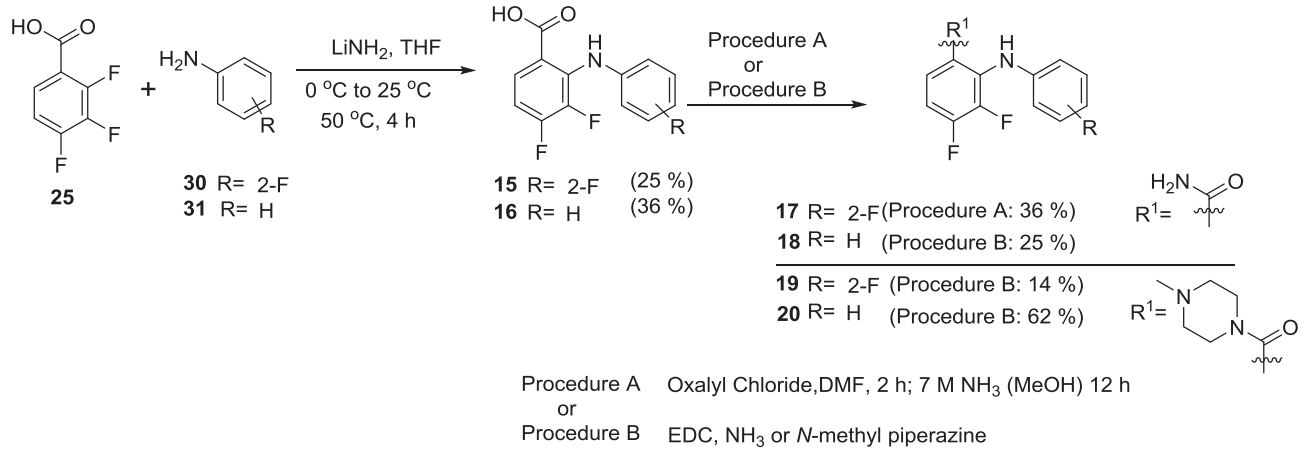

Scheme 3. Synthesis of right aryl derivatives and associated side-chain variants.

base to abstract the aniline proton and direct an *ortho* S_NAr attack on **25**.

Subsequent amide formation was achieved either by conversion to the acyl chloride then addition of the amine to yield the amide in the case of **17** where ammonia was used, or were prepared with carbodiimide couplings in the case of **18–20**. The use of EDC facilitated product isolation (See Scheme 3).

Attempts to effect conversion from the *N,N*-diphenylaniline **2** or **3** to the corresponding tertiary aniline **22** *via* an Eschweiler-Clarke conversion failed. Alkylation of the *N,N*-diphenylaniline with methyl iodide and sodium hydride in DMF was also unsuccessful. Reductive alkylation of the aniline precursor, 2-fluoro-4-iodoaniline (**26**), preceded in acceptable yield to give the mono *N*-methylated product, **35**, shown in Scheme 4.[52,53] This secondary aniline was then added into 2,3,4-trifluorobenzoic acid (**25**) using the standard S_NAr lithium amide displacement approach of Davis.[45] Conversion to the desired final compounds followed the previously described acyl chloride route (See Scheme 5).

The use of intact cells rather than isolated enzymes was selected as the primary screen for several reasons. First, native signaling cascades require multiple kinase events initiated by an external ligand binding event; this initial event can be reproduced reliably *in vitro* with the use of EGF. Notably triple-negative breast cancer cells can be used directly and may be predictive of activity in actual tumors. Second, MEK1/2 or MEK5 must be activated by dual phosphorylation to its active form to be catalytically active. This would require either *in vitro* conversion of the wild-type MEK to the active form by a second enzyme (MEKK) or the use of a constitutively active MEK5βDD mutant. Although affinity for the isolated enzyme is potentially useful information, the unavailability of isolated MEK5 protein of either variety (MEK5 or MEK5DD), but more significantly extensive protein-protein interactions[31] of MEK5 with ERK5 recommend an isolated enzyme may not perfectly represent *in vivo* conditions. Consequently, the cellular assay is proposed as better representing actual physiological conditions. The significant molecular weight difference of the final antibody-identifiable phospho proteins pERK1, pERK2, and pERK5 (MW: pERK1: 43.4 kDa: pERK2: 41.4 kDa; pERK5: 88.4 kDa) permits efficient analysis of inhibition of the various MEK/ERK cascades simultaneously. More rigorous confirmation of engagement at the level of MEK and more significantly as type III inhibitors will require additional studies on compounds identified in these initial screens. The compounds were initially examined in triplicate at a single concentration of 10 μM on EGF-stimulated triple-negative breast cancer MDA-MB-231 cells. Controls included DMSO as the blank representing 100% activity, and compound activity is represented as percent decrease in activity normalized to the DMSO blank. EGF stimulates both the MEK1/2 cascades as well as the MEK5 cascade and acted as a control to confirm intact signaling cascades. Standard compounds included U0126, a compound known to inhibit MEK1 and other kinases not including MEK5. U0126 is not competitive with ATP although the precise site of U0126 inhibition remains unconfirmed. XMD8-92 was originally prepared the Gray lab[10] and is an ATP-site inhibitor of ERK5 and used as the standard for inhibition of the MEK5/ERK5 cascade. Results are presented in Table 1.

Compounds **2–11** represent point variations of the sidechain with the rest of the structure unaltered. With the exception of the diethyl amide, **5**, and to a lesser extent the ethylene-lined tertiary amine, **9**, all showed good activity at inhibiting the product of MEK1/2: pERK1/2. Of the side chain variations very few showed appreciable activity at MEK5. Compounds **5** and **11** display a slight activation of MEK5 activity above 100 activity (0% inhibition) by a repeatable, yet not fully understood mechanism. Overall, this does indicate that MEK1/2 versus MEK5 selectivity may be possibly achieved by structural variation in this domain, the path toward increasing MEK5 activity selectively is not obvious with compounds **2–11** alone.

For the non-halogen central ring variations, all were considerably less active both at MEK1/2 and MEK5. The 4-*N*-methyl piperazine derivative, **14**, although not a direct comparison of **11**, did have the best activity at inhibition of MEK5 and did have the best selectivity for MEK5 versus MEK1/2 inhibition for the compounds examined so far. If any conclusion can be draw from compounds **12–14** it would be that MEK5 can tolerate a less polarized central arene better than MEK1/2.

Terminal arene variations **12–20** explored both terminal arene

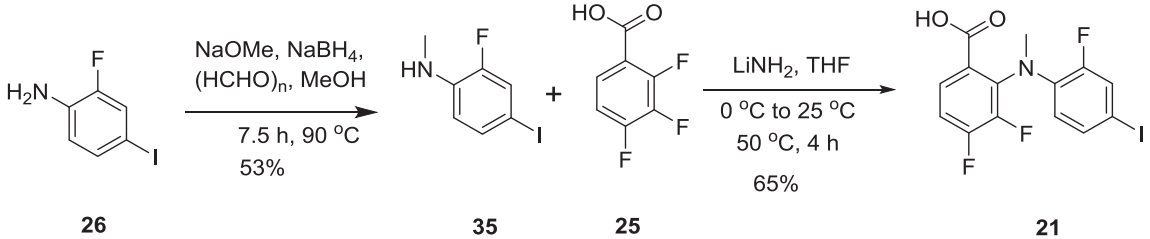

Scheme 4. Monomethylation reaction of **26** then synthesis of acid **21** by lithium amide displacement method.

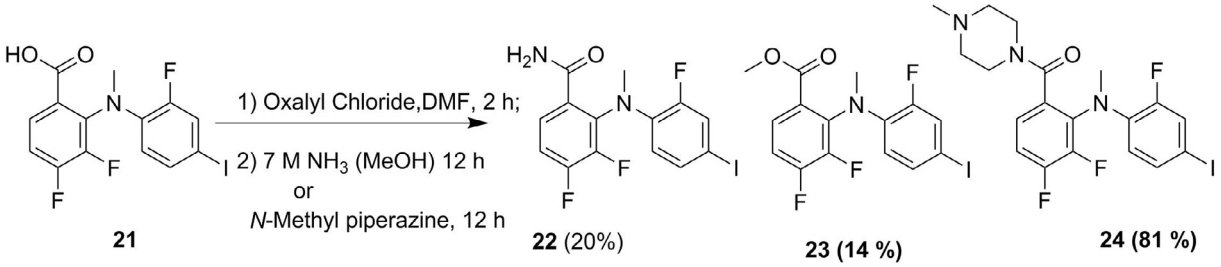

Scheme 5. Synthesis of side chain variants of *N*-Methyl derivatives.

variations and side chain variations with the central ring held constant with a 3,4-difluorophenyl substitution pattern. Activity was variable across these series. When the carboxylate side chain compounds **2**, **15**, and **16** are compared, the point omission of the 4-iodo generates compounds that are half as active at inhibiting the MEK1/2 cascade and are devoid of MEK5 inhibition. The amides present a more complicated profile when the terminal arene is modified. For the primary amides **3**, **17**, and **18**, MEK1/2 activity is only moderately reduced with the omission of the 4-iodo. Removal of both the 2-fluoro atom and the 4-iodo atom generates much weaker MEK1/2 inhibitors, approximately one third of the fully adorned lead, compound **3**. For the primary amides, MEK5 activity is weak across the board. The piperazine of the terminal arene series **10**, **11**, **19**, and **20** identify compounds **20** as the most potent and most selective at MEK5. The high activity at MEK5 of the fully dehalogenated terminal arene **20** bearing a cationic charge contrasts to the neutral primary amide series and the anionic carboxylic series with the equivalent terminal arene substitution pattern. This suggests that the cationic piperazine, in the case of MEK5 inhibitors, may contribute more than halogen interactions of the terminal ring.

Preventing internal hydrogen bonding by replacing the aniline *N*-H with an aniline *N*-methyl has differential effects on MEK1/2 versus MEK5 activity. Comparison of **2** with **21** indicates that if the carboxylate is prevented from internal hydrogen/ionic bonding the compound is much more potent at inhibiting of MEK1/2 than MEK5. The relatively

Table 1
MEK1/2 and MEK inhibition data.

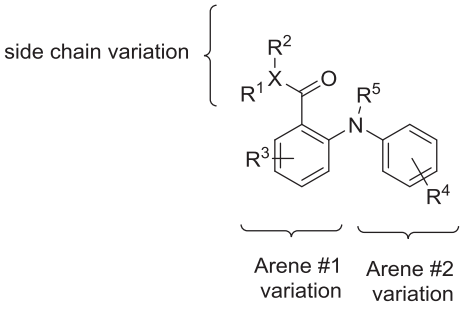

Compound	Side chain (R^1R^2X)	Central ring (R^3)	Terminal ring (R^4)	Nitrogen substitution (R^5)	Decrease in pERK1/2	Decrease in pERK5
2	HO	3-F,4-F	2-F,4-I	H	98.5	20.1
3	H_2N	3-F,4-F	2-F,4-I	H	96.8	59
4	Me_2N	3-F,4-F	2-F,4-I	H	87.3	0.2
5	Et_2N	3-F,4-F	2-F,4-I	H	5.5	0*
6	MeHN	3-F,4-F	2-F,4-I	H	99.6	20.4
7	MeO	3-F,4-F	2-F,4-I	H	98.9	13
8	EtHN	3-F,4-F	2-F,4-I	H	98.6	8.5
9	$Me_2N(C_2H_4)MeN$	3-F,4-F	2-F,4-I	H	27.9	9.4
10	BOC-Piperazine	3-F,4-F	2-F,4-I	H	70.9	8.4
11	Piperazine	3-F,4-F	2-F,4-I	H	99	0*
12	H_2N	–	2-F	H	0*	39
13	4-methylpiperazine	–	2-F,4-I	H	33.5	30.9
14	4-methylpiperazine	–	–	H	29.3	71
15	HO	3-F,4-F	2-F	H	31.7	0*
16	HO	3-F,4-F	–	H	43.5	0*
17	H_2N	3-F,4-F	2-F	H	80.2	24.5
18	H_2N	3-F,4-F	–	H	35.3	14.8
19	4-methylpiperazine	3-F,4-F	2-F	H	37.1	56.1
20	4-methylpiperazine	3-F,4-F	–	H	0*	82.4
21	HO	3-F,4-F	2-F,4-I	Me	67.1	18.4
22	H_2N	3-F,4-F	2-F,4-I	Me	73	0*
23	MeO	3-F,4-F	2-F,4-I	Me	50.9	91.6
24	4-methylpiperazine	3-F,4-F	2-F,4-I	Me	0*	27.2
Blank	–	–	–		0	0
PD 0325901					99.7	95.9
U0126					99.6	43
XMD8-92					50.1	95.2

0* = moderate (~20%) increase of pERK identified.

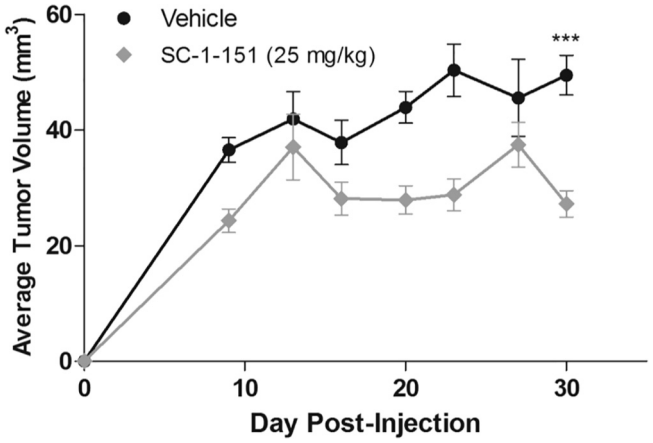

Fig. 10. Compound **3** (SC-1-151) inhibits MDA-MB-231 tumorigenesis *in vivo*.

high activity of the ester **23** requires additional examination to understand increased activity of **23** selectively for MEK5 when contrasted to the activity of **21**. Given similar MEK1/2 activity between **12** and **23**, it is unlikely to result from differential transport. Piperazine **24** compared to piperazine **11** was much weaker for MEK1/2. The MEK5 activity was less for compound **24** than **20**. This remarkable loss of activity could arise from a lack of directionality of the cation when internal hydrogen bonding is prevented by the aniline methyl. Piperidine derivatives with an internal hydrogen bond (compounds **20**, **14**, and **11**) may represent a very favorable placement of the cationic nitrogen. When compound **20** was overlaid on the ligand of 3EQC or on the proposed ligand binding site of the MEK5 homology models, the basic amine of the piperazine rotated through a region of space that was 4 Angstroms within the aspartic acid carboxylates of the HRD sequences of MEK1 and MEK5, Asp190 and Asp283 respectively. Additionally the *N*-methylpiperazine when directed by internal H-bonding and the pyamidalized amide nitrogen can exist within H-bonding interaction (3 Å) of the Tyr315 reside of the YVGT of MEK5 or the corresponding Phe223 of MEK1.

Testing MEK inhibitors for efficacy in a tumor xenograft was essential to confirm any validity to the idea that MEK and perhaps MEK5 may be relevant for actual tumors. Compound **3** was selected as it was one of the earliest compounds identified to display significant MEK5 inhibition. Severe Combined Immune Deficient SCID/beige female mice with a MDA-MB-231/matrigel xenograft were treated with either DMSO or compound **3** (SC-1-151) (25 mg/kg) for 31 days. Tumor volume in the group treated with compound **3** was significantly lower than that of DMSO-treated animals at day 30 post cell injection (29.10 mm^3 ± 2.29 SEM and 49.48 mm^3 ± 3.44 SEM, respectively, p-value = 0.0001), implicating the role of dual MEK1/2 and MEK5 inhibition on tumor growth (See Fig. 10).

In summary, there does appear to be the possibility to develop MEK isoform-selective small molecules that are active against intact MEK/ERK signaling cascades and may have relevance to *in vivo* tumors. There appears to be divergent structure-activity correlations for compounds with carboxylate, neutral, or cationic resides on the side chain. These ionic effects appear to predominate over terminal arene hydrophobic and halogen contributions to activity. Specifically in the *N*-methyl-bound piperazine series, compound **20**, displayed both potency and selectivity for inhibition of the MEK5/ERK5 cascade despite having no halogens on the terminal arene. This suggests that altering hydrophobic properties of the lead compound **3** (cLogP = 4.4) may be consistent with improving both PD and PK properties in a parallel direction as exemplified by compound **20** (cLogP = 3.6). The differential activity of tertiary aniline compounds are also consistent with diverging activity profiles for sidechains with a positive versus a negative charge. The positioning of a cationic amine in a favorable orientation (by internal hydrogen bonding) appears more significant than halogen bonding from the terminal arene. This raises the possibility that the pharmacokinetically unfavorable 4-iodine atom may be dispensable for MEK5 activity in rotationally-restricted compounds with a cationic side chain. In contrast, freely rotating *N,N*-diphenylaniline carboxylates seem to favor MEK5 selectivity but this will require additional validation.

A. Supplementary data

Supplementary data associated with this article can be found, in the online version, at http://dx.doi.org/10.1016/j.bmcl.2018.05.029.

References

1. Drew BA, Burow ME, Beckman BS. *BBA.* 2012;1825:37.
2. Endicott JA, Noble MEM, Johnson LN. *Annu Rev Biochem.* 2012;81:587.
3. Tian T, Harding A. *Cell Cycle.* 2014;13:2379.
4. Harding A, Tian T, Westbury E, et al. *Curr Biol.* 2005;15:869.
5. Kim EK, Choi E-J. *Arch Toxicol.* 2015;89:867.
6. Simoes AES, Rodrigues CMP, Borralho PM. *Drug Discov Today.* 2016;21:1654.
7. Giurisato E, Tournier C, Giurisato E. *Cell Cycle.* 2016;15:619.
8. Hoang VT, Yan TJ, Cavanaugh JE. *Cancer Lett (NY., NY, US).* 2017;392:51.
9. Anon. Cancer Discovery 2014, 4, 1363.
10. Deng X, Yang Q, Kwiatkowski N, et al. *ACS Med Chem Lett.* 2011;2:195.
11. Wang J, Li Q, Wang C, et al. Biochem Pharmacol (Amsterdam, Neth.). 2016;99:132.
12. Honda T, Obara Y, Yamauchi A, et al. *PLoS ONE.* 2015;10 e0117914/1.
13. Raviv Z, Kalie E, Seger R. *J Cell Sci.* 2004;117:1773.
14. English JM, Pearson G, Hockenberry T, et al. *J Biol Chem.* 1999;274:31588.
15. Kamakura S, Moriguchi T, Nishida E. *J Biol Chem.* 1999;274:26563.
16. Barros JC, Marshall CJ. *J Cell Sci.* 2005;118:1663.
17. Lochhead PA, Gilley R, Cook SJ. *Biochem Soc Trans.* 2012;40:251.
18. Hsieh FC, Cheng G, Lin J. *Biochem Biophys Res Commun.* 2005;335:292.
19. Montero JC, Ocana A, et al. *PLoS ONE.* 2009;4:e5565.
20. Ohren JF, Chen H, Pavlovsky A, et al. *Nat Struct Mol Biol.* 2005;12:278.
21. Sebolt-Leopold JS, English JM. *Nature (London, UK).* 2006;441:457.
22. Gavrin LK, Saiah E. *MedChemComm.* 2013;4:41.
23. Palmieri L, Rastelli G. *Drug Discovery Today.* 2013;18:407.
24. Tatake RJ, O'Neill MM, Kennedy CA, et al. *Biochem Biophys Res Commun.* 2008;377:120.
25. Kolar MH, Hobza P. *Chem Rev (Washington, DC, US.).* 2016;116:5155.
26. Ford MC, Ho PS. *J Med Chem.* 2016;59:1655.
27. Persch E, Dumele O, Diederich F. *Angew Chem Int Ed.* 2015;54:3290.
28. Wilcken R, Zimmermann MO, Lange A, et al. *J Med Chem.* 2013;56:1363.
29. Grant SK, Lunney EA. *Chem Biol (Cambridge, MA, US).* 2011;18:3.
30. Heald RA, Jackson P, Savy P, et al. *J Med Chem.* 2012;55:4594.
31. Glatz G, Gógl G, Alexa A, et al. *J Biol Chem.* 2013;288:8596.
32. Fischmann TO, Smith CK, Mayhood TW, et al. *Biochemistry.* 2009;48:2661.
33. English JM, Vanderbilt CA, Xu S, et al. *J Biol Chem.* 1995;270:28897.
34. Khokhlatchev A, Xu S, English J, et al. *J Biol Chem.* 1997;272:11057.
35. Cameron SJ, Abe J-I, Malik S, et al. *J Biol Chem.* 2004;279:1506.
36. Spicer JA, Rewcastle GW, Kaufman MD, et al. *J Med Chem.* 2007;50:5090.
37. Bariwal J, Van der Eycken E. *Chem Soc Rev.* 2013;42:9283.
38. Beletskaya IP, Cheprakov AV. *Organometallics.* 2012;31:7753.
39. Vachhani DD, Kumar A, Modha SG, et al. *Eur J Org Chem.* 2013;2013:1223.
40. Pericherla K, Jha A, Khungar B, et al. *Org Lett.* 2013;15:4304.
41. Majumdar KC, Ganai S. *Tetrahedron Lett.* 2013;54:6192.
42. Kaswan P, Pericherla K, Kumar A. *Synlett.* 2013;24:2751.
43. Zhou F, Guo J, Liu J, et al. *J Am Chem Soc.* 2012;134:14326.
44. Tan G, Yang Y, Chu C, et al. *J Am Chem Soc.* 2010;132:12231.
45. Davis EM, Nanninga TN, Tjiong HI, et al. *Org Process Res Dev.* 2005;9:843.
46. El-Faham A, Albericio F. *Chem Rev (Washington DC US).* 2011;111:6557.
47. Gaedda TM, Kawanishi Y, Miyazawa A. *Synth Commun.* 2012;42:1259.
48. Vera-Luque P, Alajarin R, Alvarez-Builla J, et al. *Org Lett.* 2006;8:415.
49. Pellon RF, Martin A, Mesa M, et al. *J Chem Res.* 2006:527.
50. D'Angelo ND, Peterson JJ, Booker SK, et al. *Tetrahedron Lett.* 2006;47:5045.
51. Martin A, Pellon RF, Mesa M, et al. *J Chem Res.* 2005:561.
52. Teichert A, Jantos K, Harms K, et al. *Org Lett.* 2004;6:3477.
53. Barluenga J, Bayon AM, Asensio G. *J Chem Soc Chem Commun.* 1984:1334.